Elsevier Editorial System(tm) for Journal of

the European Ceramic Society

Manuscript Draft

Manuscript Number: JECS-D-19-00728R1

Title: Thermophysical property and electrical conductivity of titanium

isopropoxide - polysiloxane derived ceramics

Article Type: Full Length Article

Keywords: Silicon oxycarbide; Titanium carbide; Phase Evolution; Thermal

stability; Electrical conductivity.

Corresponding Author: Professor Kathy Lu, PhD

Corresponding Author's Institution: Virginia Tech

First Author: Ni Yang

Order of Authors: Ni Yang; Kathy Lu, PhD

Abstract: In this study, high temperature resistant Si-O-C-Ti has been successfully prepared based on the pyrolysis of polysiloxane (PSO) and titanium (IV) isopropoxide (TTIP) at 1200-1400 °C. PSO can homogeneously mix with TTIP to enhance its conversion to TiC. The carbothermal reactions between TiO2 (product of thermal decomposition of TTIP) and carbon result in the formation of TiC. All the Si-O-C-Ti composites pyrolyzed at 1200-1300 °C are stable up to 1000 °C in an oxidizing air atmosphere. TiC leads to high electrical conductivity at elevated temperatures; the maximum conductivity is 1176.55 S/m at 950 °C, which is the first reported value of >1000 S/m conductivity for Si-O-C-Ti ceramics. However, too high a pyrolysis temperature, such as 1400 °C, can potentially 'destabilize' the Si-O-C-Ti system by consuming the free carbon and result in lower conductivities.

Research Data Related to this Submission

\_\_\_\_\_

There are no linked research data sets for this submission. The following reason is given:

Data will be made available on request

\*Summary of Novel Conclusions

# **Sumary of Novel Conclusions**

Thermophysical Property and Electrical Conductivity of Titanium Isopropoxide – Polysiloxane Derived

Ceramics

Ni Yang, Kathy Lu\*

Department of Materials Science and Engineering, Virginia Polytechnic Institute and State
University, Blacksburg, Virginia, 24061,USA

\*Corresponding author: Email: klu@vt.edu

High temperature stable Si-O-C-Ti ceramic with the highest electrical conductivity of 1176.55 S/m at 950 °C has been synthesized by pyrolysis of polysiloxane and titanium (IV) isopropoxide at 1300 °C.

Thermophysical Property and Electrical Conductivity of Titanium Isopropoxide –

Polysiloxane Derived Ceramics

Ni Yang, Kathy Lu\*

Department of Materials Science and Engineering, Virginia Polytechnic Institute and State
University, Blacksburg, Virginia, 24061,USA

\*Corresponding author: Email: klu@vt.edu

**Declarations of interest**: none

**Abstract** 

In this study, high temperature resistant Si-O-C-Ti has been successfully prepared based on the pyrolysis of polysiloxane (PSO) and titanium (IV) isopropoxide (TTIP) at 1200-1400 °C. PSO can homogeneously mix with TTIP to enhance its conversion to TiC. The carbothermal reactions between TiO<sub>2</sub> (product of thermal decomposition of TTIP) and carbon result in the formation of TiC. All the Si-O-C-Ti composites pyrolyzed at 1200-1300 °C are stable up to 1000 °C in an oxidizing air atmosphere. TiC leads to high electrical conductivity at elevated temperatures; the maximum conductivity is 1176.55 S/m at 950 °C, which is the first reported value of >1000 S/m conductivity for Si-O-C-Ti ceramics. However, too high a pyrolysis temperature, such as 1400 °C, can potentially 'destabilize' the Si-O-C-Ti system by consuming the free carbon and result in lower conductivities.

**Keywords:** Silicon oxycarbide; Titanium carbide; Thermophysical Property; Phase Evolution; Thermal stability; Electrical conductivity

#### 1. Introduction

Based on the homogeneous mixing of starting precursors at the molecular level, polymer-derived ceramics enable the formation of homogeneous microstructures [1] and novel properties [2, 3]. One of such systems is polymer-derived silicon oxycarbide (SiOC). It is a highly adjustable system for which compositions and microstructures can be tuned vastly with different crosslinking and pyrolysis conditions. With pyrolysis temperature increase, there is a phase separation into  $SiO_2$  and then SiC domains along with free carbon formation by consuming mixed  $Si_xO_yC_z$  units [4]. Stoichiometric SiOC can be described as a network of  $SiC_{4-x}O_x$  ( $0 \le x \le 4$ ) tetrahedra units, which are randomly distributed in the SiOC system [5]. The SiOC composition can be written as  $SiC_xO_{2(1-x)} + y(C_{free}$  or  $Si_{free}$ ), which means that excess free carbon or excess free silicon can be present in the matrix. Towards this, SiOC material has been recently shown to display favorable properties for use in biomedical devices [6], metal-oxidesemiconductor devices [7], white light emitting devices [8], integrated pressure sensors [9], and anodes for lithium-ion batteries [10]. Owing to its diverse range of applications, the SiOC system is considered as one of the most promising research areas in polymer derived ceramics.

With the increasing need for functional high temperature materials, high electrical conductivity and thermal stability in harsh environments have become especially important, stimulated by their potential applications for microelectromechanical systems and advanced energy storage devices. However, the SiOC system is not a highly conductive material. Overall, the electrical conductivity provided by carbon-rich SiOC systems displays low values (~ 1 x 10<sup>-3</sup> S cm<sup>-1</sup>) [3]. In addition, the free carbon in the SiOC matrix leads to low thermal stability [2, 3, 11]. At high temperatures, carbothermal reduction in the SiOC system may result in weight loss and lead to deterioration of thermal stability. Many factors have been proven to have an effect on

the high temperature stability, such as the content of free carbon in SiOC [12], polymer precursor type [13], SiOC microstructure [14], and pyrolysis condition [12]. In our previous work [3, 15, 16], the most sensitive issues for the thermal stability of SiOCs are oxidative breakdown of the SiOC structure (above 800 °C) and oxidation of free carbon (400-800 °C).

Recently, ceramic composites from SiOC systems with fillers have been reported [15, 17-19]. Doping the Si–O–C matrix with extra elements such as B, Al, Ti, and Zr can be achieved by adding metal complexes or metal-based particles to the starting polymeric solution. In the presence of a carbide-forming transition metal (Ti, Zr, or Cr) or a transition-metal boride or silicide, the tremendous linear shrinkage encountered during the polymer pyrolysis may be drastically reduced, hence facilitating production of bulk components [14]. More importantly, the thermal stability and electrical conductivity have been improved after introducing fillers into the SiOC matrix [15, 20, 21]. For example, polymer derived SiOC/ZrO<sub>2</sub> ceramic composites have been successfully prepared by pyrolysis of polymethylsilsesquioxane and nanocrystalline ZrO<sub>2</sub> particles, and the thermal stability increases with respect to crystallization and decomposition at temperatures exceeding 1300 °C [20]. Functionalized TiO<sub>2</sub> nanoparticles promote the formation of TiC<sub>x</sub>O<sub>y</sub> in a SiOC-based composite, and achieve an electrical conductivity of 5.03 S/cm at 400 °C in air [15]. SiOC/HfO<sub>2</sub> fibers have good thermal stability with no observable weight loss up to 1500 °C, and the electrical property of the fibers is improved due to the incorporation of carbon into the SiO<sub>2</sub> network [23].

In our prior work [15], SiOC-TiC<sub>x</sub>O<sub>y</sub> ceramic has been synthesized based on the reaction between TiO<sub>2</sub> nanoparticles and free carbon in the matrix during pyrolysis. In order to enhance the dispersibility of the TiO<sub>2</sub> nanoparticles in the polymer precursor, surface-modification has been carried out on the TiO<sub>2</sub> particles by surfactant sodium dodecyl sulfate (SDS). The SiOC

ceramic containing the surface-modified TiO<sub>2</sub> has the highest electrical conductivity (~5.03 S/cm) compared to the TiO<sub>2</sub>-SiOC ceramic without the TiO<sub>2</sub> surface modification (~3.07 S/cm) in air, which proves the important effect of homogeneous dispersion of additives on the electrical properties. However, the surface chemistry incompatibility between the additives and the polymer precursor is still difficult to address because one is hydrophilic (such as the hydroxyl groups on the TiO<sub>2</sub> surface) and the polysiloxane precursors are hydrophobic [24]. Meanwhile, small size TiO<sub>2</sub> additives, such as nanoparticles, have a significant tendency of aggregation due to the high surface area. Inhomogeneous distribution of TiO<sub>2</sub> nanoparticles in the matrix, especially with increasing TiO<sub>2</sub> content, can lead to lower thermal stability.

In this study, titanium (IV) isopropoxide (TTIP) has been incorporated into phenyl and methyl containing polysiloxane to develop Si-O-C-Ti composites. The effects of the additive filler content and pyrolysis temperature on the phase evolution as well as thermophysical and electrical properties are systematically investigated. The mechanisms for phase transformation that lead to superior electrical and thermal behavior of SiOC/TiC ceramic are proposed and discussed on the basis of Raman spectroscopy, XRD (X-ray diffraction), XPS (X-ray photoelectron spectroscopy), TGA (thermogravimetric analysis), and HRTEM (High-resolution transmission electron microscopy).

## 2. Experimental procedure

Commercial polysiloxane Polyramic<sup>®</sup> SPR-684 (PSO, [-Si(C<sub>5</sub>H<sub>6</sub>)<sub>2</sub>O-]<sub>3</sub>[-Si(CH<sub>3</sub>)(H)O-]<sub>2</sub>[-Si(CH<sub>3</sub>)(CH=CH<sub>2</sub>)O-]<sub>2</sub>, Starfire Systems, Inc., Schenectady, NY) was used as the polymer precursor. Titanium (IV) isopropoxide (TTIP, Ti(OCH(CH<sub>3</sub>)<sub>2</sub>)<sub>4</sub>, Acros, NJ) with 98+% purity was chosen as the titanium-containing additive. 2.1-2.4 % platinum divinyltetramethyldisiloxane

complex in xylene (Pt catalyst, Gelest Inc., Morrisville, PA) diluted with toluene was used as a hydrosilylation catalyst.

TTIP/PSO mixtures with the corresponding Ti to Si molar ratios of 0.05, 0.10, 0.15, and 0.20 (marked as SiOC-Ti=0.05, SiOC-Ti=0.10, SiOC-Ti=0.15, and SiOC-Ti=0.20 respectively) were prepared in an argon atmosphere in a glove box (Labstar<sup>pro</sup>, MBRAUN<sup>®</sup>, Stratham, NH). During vigorous stirring of the above mixtures at 250 rpm, 2.5 ppm of the diluted Pt catalyst solution was slowly added to the mixtures. After the mixture was stirred for 30 min, the homogeneous mix was poured into cylindrical aluminum molds and placed in a vacuum chamber at 1500 mTorr to remove all the bubbles. Before crosslinking, the mixture was a yellowish yet transparent liquid without any bubbles. After curing at 50 °C for 12 h and 100 °C for 24 h in an oven, the cross-linked sample was hard, black, and crack—free. The cured samples were cut and polished to roughly 10 mm x 10 mm x 1.5 mm size and placed in zirconia boats with both sides covered by graphite mats before putting into a tube furnace (1730 – 12 Horizontal Tube Furnace, CM Furnaces Inc., Bloomfield, NJ) for pyrolysis. The samples were heated up to 1200 °C, 1300 °C, and 1400 °C at a rate of 1 °C/min with 2 h holding and cooled down to 50 °C with a rate of 2 °C/min. The ceramic yield and shrinkage of the above samples were recorded.

The density of the resulting products was measured in triplicate by a pycnometer (AccuPyc II 1340, Micromeritics<sup>®</sup>, Norcross, GA), using helium gas at an outlet pressure of 1.34 bars in a 7.8 cm<sup>3</sup> sample cell. Phase compositions of the pyrolyzed samples were examined using an X'Pert PRO diffractometer (PANalytical B.V., EA Almelo, The Netherlands). Rietveld refinement of the diffraction data was performed using X'Pert HighScore Plus. JCPDS cards 98-001-2065 and 98-009-3040 were used to index SiC and TiC phases, respectively. The thermal stability of the samples after pyrolysis was analyzed by thermogravimetric analysis (TGA) using

a STA 449C Jupiters® analyzer (Netzsch - Gerätebau GmbH, Selb, Germany) from room temperature to 1000 °C at a heating rate of 10 °C/min and an air flux of 40 ml/min as well as in a furnace at 1000 °C in air for up to 100 h. The electrical conductivity of the pyrolyzed samples was measured from 50 °C to 1200 °C in an Ar atmosphere with a four-point probe configuration from a potentiostat (Versa STAT 3, Princeton Applied Research, Oak Ridge, TN). For the conductivity measurements, silver/palladium paste (ESL Electroscience, PA, USA) electrodes were painted on the surfaces of the specimens. Raman spectra were recorded on a Horiba spectrometer (JY Horiba HR 800) with an excitation wavelength of 514 nm produced by an Ar laser between the spectral range of 250–3500 cm<sup>-1</sup>. The microstructures of the pyrolyzed ceramics were studied using a transmission electron microscope (JEOL 2100, JEOL USA, Peabody, MA); the TEM samples were prepared by grinding the pyrolyzed samples in a mortar and then dispersing them in absolute methanol. Chemical compositions were examined by X-ray photoelectron spectroscopy (XPS, PHI Quantera SXM) equipped with an Al Kα source (1486.6 eV).

## 3. Results and discussion

## 3.1. Thermophysical properties

Table 1 displays the volume shrinkage, ceramic yield, and density of the samples after pyrolysis at 1200°C, 1300°C, and 1400°C. All the pyrolyzed samples are light-reflecting black and maintain good shapes and high integrity. The pure SiOC sample shows no distinction in physical appearance vs. the Si-O-C-Ti samples.

Table 1. Volume shrinkage, ceramic yield, and density of the pyrolyzed samples.

9	Samples	Volume shrinkage (%)			Ceramic yield (%)			Density (g/cm <sup>3</sup> )		
L 2 3	zumpr <b>e</b> s	1200°C	1300°C	1400°C	1200°C	1300°C	1400°C	1200°C	1300°C	1400°C
4 5 6	SiOC	40.35±	47.29±	45.25±	83.34±	81.22±	74.59±	1.64±0.52	1.77±0.24	1.84±0.04
6 7 3		2.47	0.37	1.10	4.23	5.28	0.54	1.0.1-0.52	1.7, -0.2	1.0.001
	SiOC-Ti-	41.04±	49.78±	46.65±	76.56±	74.15±	74.21±	1.81±0.30	1.84±0.42	1.87±0.10
1 2 3	0.05	1.50	0.51	0.89	0.07	0.42	1.19	1.01±0.30	1.04±0.42	1.67±0.10
	SiOC-Ti-	50.66±	55.06±	52.53±	71.24±	68.40±	68.39±	1.86±0.42	1.91±0.33	1.93±0.06
5 7 8	0.10	0.55	0.75	1.01	0.77	0.85	1.80	1.60±0.42	1.91±0.33	1.93±0.00
9	SiOC-Ti-	53.79±	58.45±	56.92±	66.67±	63.48±	63.64±	1.90±0.40	1.96±0.32	1.98±0.36
L 2 3 _	0.15	1.87	0.83	0.67	0.30	0.26	0.70	1.7040.40	1.70±0.32	1.70±0.30
4	SiOC-Ti-	64.47±	59.70±	60.58±	65.59±	61.17±	63.16±	1.96±1.12	1.99±0.47	2.01±0.15
6 7 8	0.20	0.78	0.78	0.91	0.72	1.06	1.54	1.70±1.12	1.77±0.4/	2.01±0.13

The pure SiOC sample pyrolyzed at 1200 °C shrinks at the lowest rate of ~40%. The values for all the Si-O-C-Ti samples range from 41% to 64% at three different temperatures. At the same pyrolysis temperature, the volume shrinkage increases with the TTIP content. It is believed that the thermal decomposition of TTIP into TiO<sub>2</sub> as well as the carbothermal reaction between TiO<sub>2</sub> and carbon lead to an increase in the volume shrinkage. The shrink process can be described as [25, 26]:

$$Ti(O-iC_3H_7)_4 \rightarrow TiO_2 + 4C_3H_6(g) + 2H_2O(g)$$
 (1)

$$TiO_2 + 3C \rightarrow TiC + 2CO(g)$$
 (2)

Table 1 also shows that the volume shrinkage steadily increases with the TTIP content, when the pyrolysis temperature is constant. For the same TTIP content, the volume shrinkage does not have a consistent trend from 1200 °C to 1400 °C. In general, it increases from 1200 °C to 1300 °C and then decreases from 1300 °C to 1400 °C. This is because Eq. (2) reacts more completely at higher temperatures, which results in larger volume shrinkage because of the evaporation of the volatile CO gas.

The ceramic yield values for all the samples in Table 1 range from 61–83%. At the same pyrolysis temperature, the ceramic yield decreases with the increase of the TTIP content. Among them, the pure SiOC samples has the highest ceramic yield (83%, 81%, and 75%) at pyrolysis temperatures of 1200 °C, 1300 °C, and 1400 °C. This is understandable as the mass loss of the pure SiOC is only dependent on the polymer decomposition. However, for the Si-O-C-Ti samples, the thermal decomposition of both the PSO and TTIP causes mass loss, especially with the consideration of the TiO<sub>2</sub> to TiC conversion (CO gas escape). More TTIP leads to more mass loss. At the same TTIP concentration, the ceramic yield generally decreases as the pyrolysis temperature increases because of the formation of more free carbon in the matrix and potentially more evaporative species (CO, CO<sub>2</sub>, etc.).

The densities for all the SiOC and Si-O-C-Ti samples are in the range of 1.64–2.01 g/cm<sup>3</sup>. At 1200 °C, as the TTIP content increases, the density slightly increases. This is because more TTIP introduces more Ti into the samples. When the pyrolysis temperature increases from 1200 °C to 1400 °C, more TiO<sub>2</sub> (4.23 g/cm<sup>3</sup>) converts into TiC (4.93 g/cm<sup>3</sup>), the density values for both of these species are much higher than those of SiOC (2.2-2.3 g/cm<sup>3</sup>), SiO<sub>2</sub> (2.65 g/cm<sup>3</sup>), and SiC (3.21 g/cm<sup>3</sup>).

#### 3.2. Phase Evolution

Fig. 1 shows the phase evolution of the SiOC matrix with different TTIP content for different pyrolysis temperatures.

At 1200 °C (Fig. 1(a)), the broad 22.9° hump corresponds to the (022) plane of amorphous SiO<sub>2</sub>. The weak and poorly defined peak at 41.4° means that the SiC content is low, consistent with typical SiOC systems. For the Si-O-C-Ti samples, some minor peaks appear at 36°, 41°, and 60°, consistent with the formation of TiC and SiC. With an increasing molar ratio of Ti to Si to 0.10, 0.15, and 0.20, these above-mentioned three peaks become stronger, an indication of more TiC and/or SiC formation. For the TiC formation, the reaction paths are shown in Eqs. (1) and (2), which is consistent with the presence of the Ti-C bonds (Ti2p, 460.7 eV) in the SiOC-Ti-0.20 pyrolyzed at 1200 °C (Fig. 2(b)). At the same time, the Si-C bonds shown in Fig. 4(a) are more related to the SiOC tetrahedrals than to SiC crystallites. The main peak of Si2p from the SiOC-Ti-0.20 system with a binding energy of 102.4 eV is attributed to the combined contribution of Si-C and Si-O bonds [27], thus the amorphous SiOC phase in the SiOC-Ti system. No SiC peak is detected for the SiOC-Ti-0.20 sample at 1200 °C and only a very small amount of SiC is observed at 1400 °C pyrolysis temperature. It is believed that the 36°, 41°, and 60° peaks in Fig. 1 are more related to TiC than to SiC. The TiC content increases with the TTIP content.

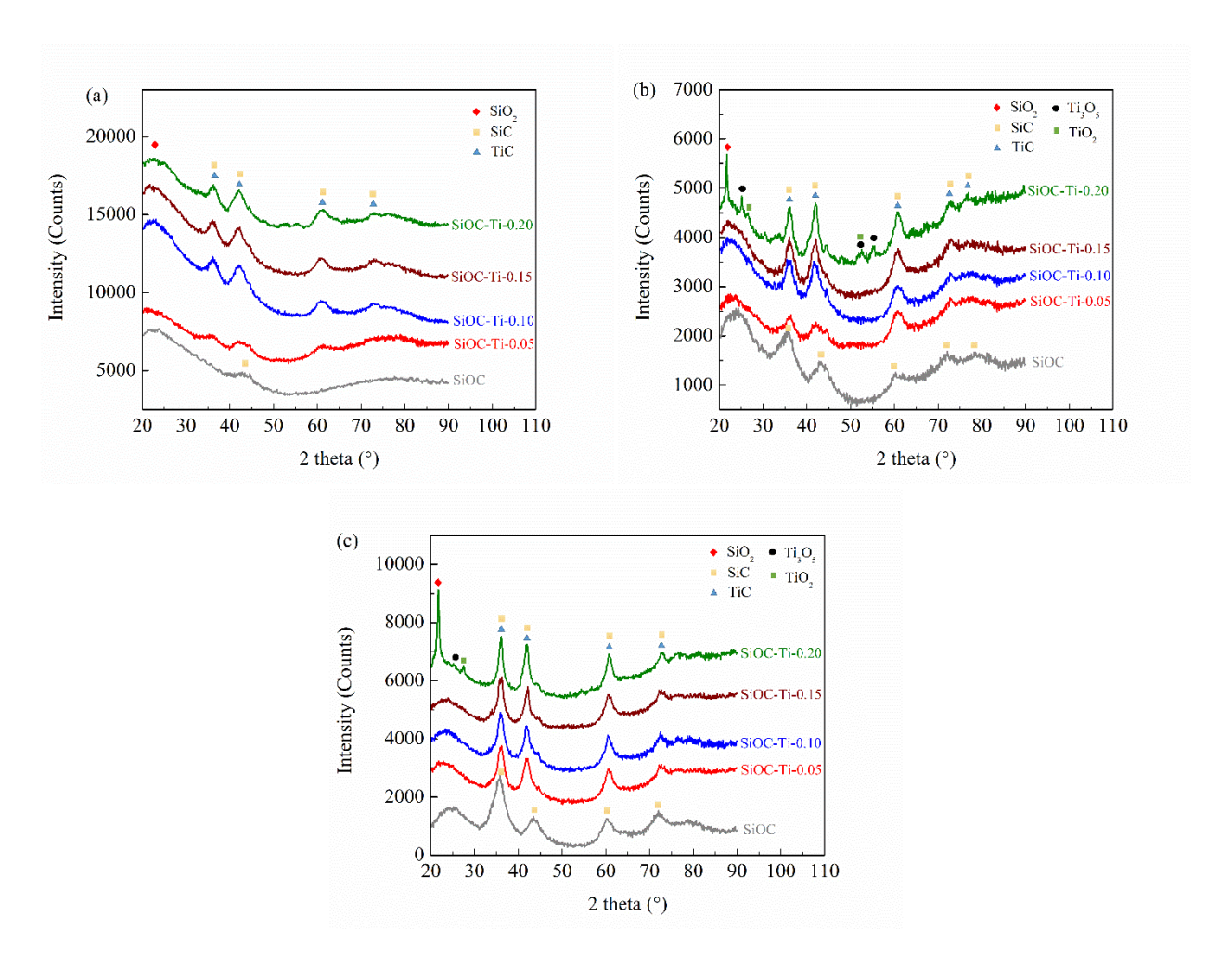


Fig. 1. XRD patterns of the SiOC samples with different amount of TTIP additive after pyrolysis at (a) 1200°C, (b) 1300°C, and (c) 1400 °C for 2 h in flowing argon.

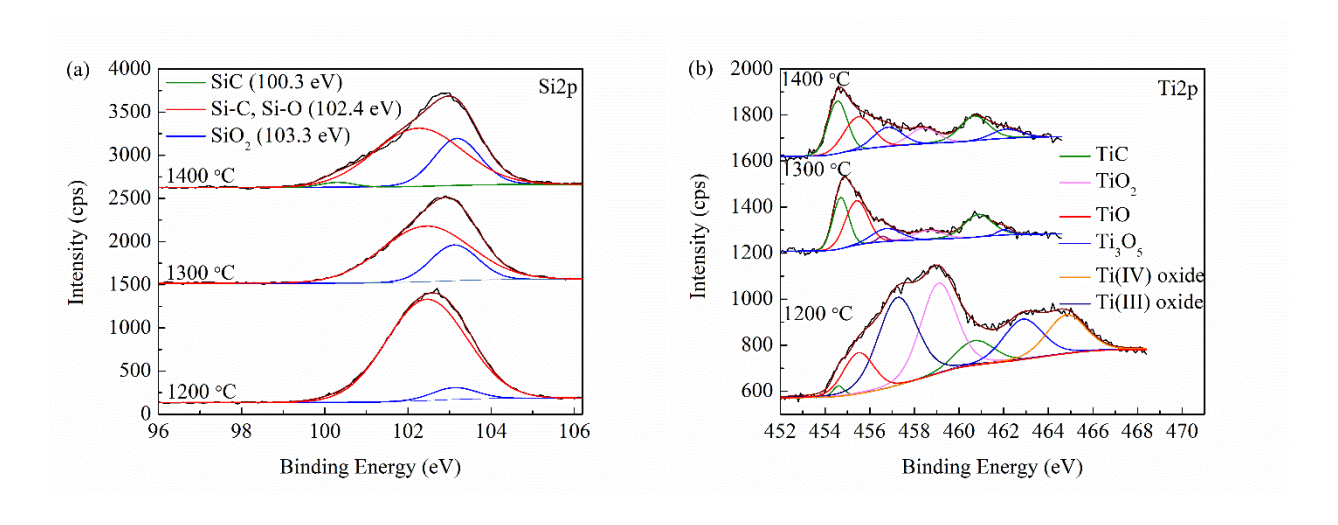


Fig. 2. XPS spectra of the SiOC-Ti-0.20 sample pyrolyzed at 1200, 1300, and 1400 °C showing the Si2p and Ti2p peaks.

With the pyrolysis temperature increase to 1300°C (Fig. 1(b)), the 35.7°, 41.4°, 60.0°, 71.8°, and 75.5° peaks corresponding to the (111), (002), (022), (113), and (222) planes of β-SiC are clearly observed for the pure SiOC sample. Also, the SiO<sub>2</sub> phase crystallizes, demonstrated by the 22.9° hump change to a sharper peak. This means that higher pyrolysis temperature accelerates the formation of SiC and the crystallization of SiO<sub>2</sub> in the SiOC matrix. With the increase of the TTIP addition, due to the consumption of carbon by TiO<sub>2</sub> through Eq. (3), the inhibiting effect from excessive carbon for the SiO<sub>2</sub> formation is decreased [15]; large SiO<sub>2</sub> domain sizes lead to the crystallization of SiO<sub>2</sub>. With the TTIP addition (Fig. 2b), the peaks for the mixture of TiC and SiC (largely TiC) centered at 36°, 41°, 60°, 72°, and 76° are more intensive. For the SiOC-Ti-0.20, both the XRD pattern from 20° to 60° and the deconvoluted XPS Ti2p peak show a series of small peaks. These peaks result from a series of intermediate oxides due to TiO<sub>2</sub> reduction by carbon, such as Ti<sub>3</sub>O<sub>5</sub> and TiO<sub>2</sub>, as well as TiC, which can be expressed as:

$$3\text{TiO}_2 + \text{C} \rightarrow \text{Ti}_3\text{O}_5 + \text{CO(g)} \tag{3}$$

The Gibbs free energy of the above equation can be calculated with an HSC Chemistry 6.0 software. The calculation results are shown in Fig. 3, which indicates that only when the temperature is higher than  $1100~^{\circ}\text{C}$  (1373.15K) is Eq. (3) thermodynamically possible (negative Gibbs free energy). However, there are no titanium intermediate oxides detected even at  $1200~^{\circ}\text{C}$  pyrolysis temperature. This may be due to the negligible amount of the predicted titanium oxides. Overall, higher TTIP content leads to more  $\text{Ti}_x\text{O}_y$  and TiC formation.

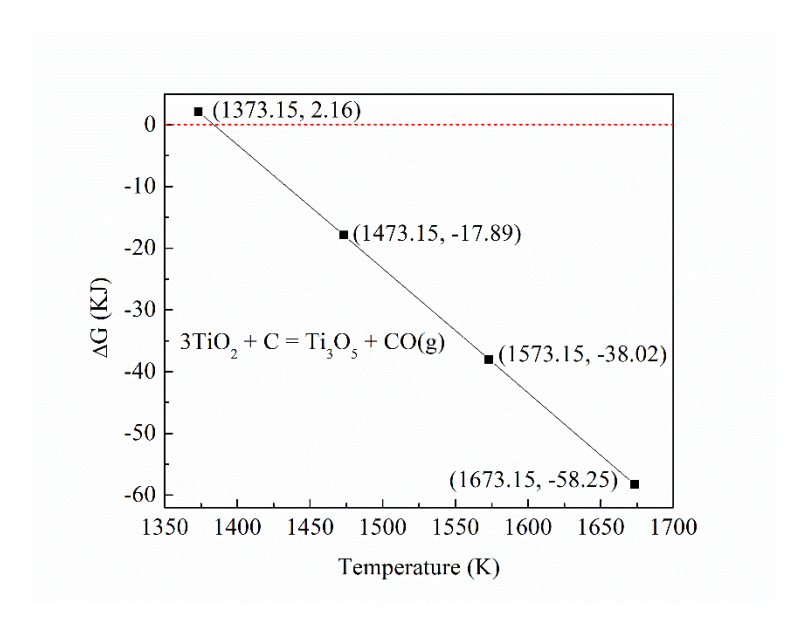


Fig. 3. Gibbs free energy versus absolute temperature for Eq. (3).

When the pyrolysis temperature is increased to 1400°C, the intense peak at 21.8° indicates tetragonal SiO<sub>2</sub> formation for the SiOC-Ti-0.20 sample. For the pure SiOC sample, there is no distinguishable difference between those of Figs. 1(b) and 1(c), except that the peaks become sharper in Fig. 1(c). As discussed, higher pyrolysis temperature increases the transition to crystalline SiO<sub>2</sub>. Nonetheless, the extent is much less than that with the TTIP addition. The XPS results in Fig. 2 also show the strengthening of the SiO<sub>2</sub> peak centered at 103.3 eV from 1200 °C to 1400 °C. The SiC formed in the matrix leads to more intense peaks in Fig. 1(c). The mechanism can be explained as:

$$SiO_2(amorphous) + 3C(graphite) \rightarrow SiC(\beta) + 2CO\uparrow$$
 (4)

The corresponding contents of TiC and SiC from the SiOC-Ti-0.05 to SiOC-Ti-0.20 samples are analyzed by Rietveld refinement. During the Rietveld refinement, several parameters are refined to generate a simulated pattern until it matches the measured profile. Table 2 lists the

contents of TiC and SiC crystalline phases. The relative weight fraction of TiC is remarkably boosted with the Ti content in SiOC.

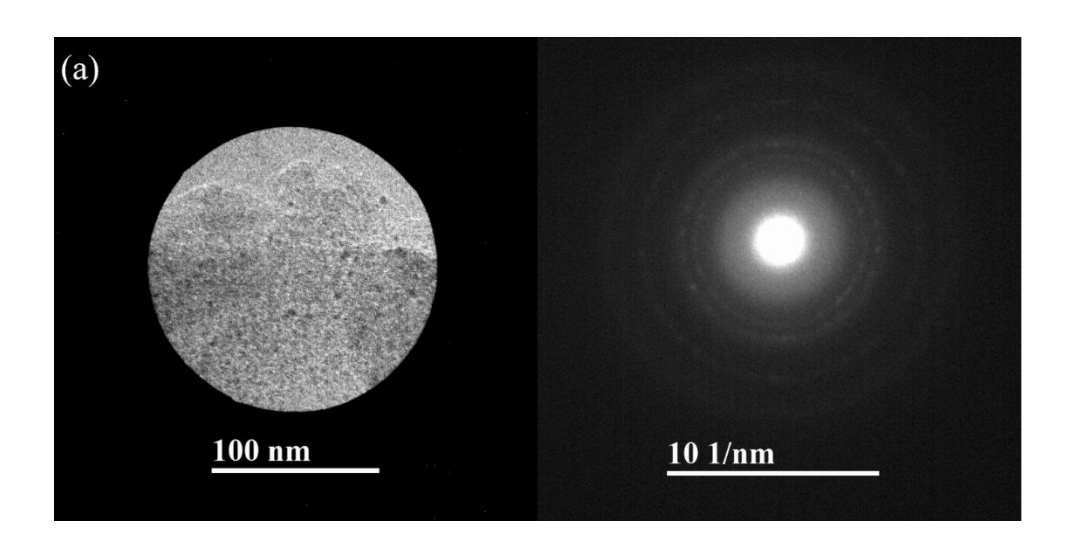
Table 2. Quantitative results of the crystalline phases by Rietveld analysis of the Si-O-C-Ti samples pyrolyzed at 1300 °C.

	Rietveld refinement (wt%)			
Sample	SiC	TiC		
SiOC-Ti-0.05	92.0	8.0		
SiOC-Ti-0.10	79.6	20.4		
SiOC-Ti-0.15	45.1	54.9		
SiOC-Ti-0.20	36.5	63.5		

As seen in Fig. 2(a), the combined contribution from the Si-C and Si-O bonds in the amorphous SiOC phase is reduced when the pyrolysis temperature goes higher. This is because more crystalline SiC and SiO<sub>2</sub> evolve from the SiOC phase. The peaks centered at 454.7 eV (Ti2p3/2) and 460.7 eV (Ti2p1/2) for TiC also become stronger from 1200 °C to 1400 °C (Fig. 2(b)), which implies the reaction conversion from titanium oxides to TiC by increasingly consuming the excessive carbon, and higher temperature promotes the extent of this reaction.

From the XRD patterns in Fig. 1, it can be concluded that crystallization of SiC and TiC starts at 1300 °C pyrolysis temperature. Fig. 4(a) shows the electron diffraction pattern of the SiOC-Ti-0.20 samples pyrolyzed at 1300 °C. Because of the amounts of the crystalline phases (e.g. SiC, TiC) are too small, the diffraction spots for these phases are not obvious. The electron diffraction pattern mainly displays the amorphous nature for the SiOC samples. The halo rings

are believed to be from the amorphous carbon and SiOC, which should be widely present [28]. In order to further distinguish the TiC and SiC phases in SiOC matrix, the high magnification microstructure is shown in Fig. 4(b). The width of the lattice distance is obtained by DigitalMicrograph® version 3. The results show that the lattice fringe width is 0.25 nm from both crystalline precipitates. However, the crystalline form is the same for SiC and TiC and the lattice parameters of TiC (0.249 nm) and SiC (0.251 nm) are similar, the identification between them is not definite due to the limit of the TEM measurements. The morphology of the precipitates is poorly defined, but the size is generally <5 nm. The worm-like features throughout the SiOC matrix are from the turbostratic carbon layers, which have twisted layer structures from the out-of-registry stacking of the graphene layers.



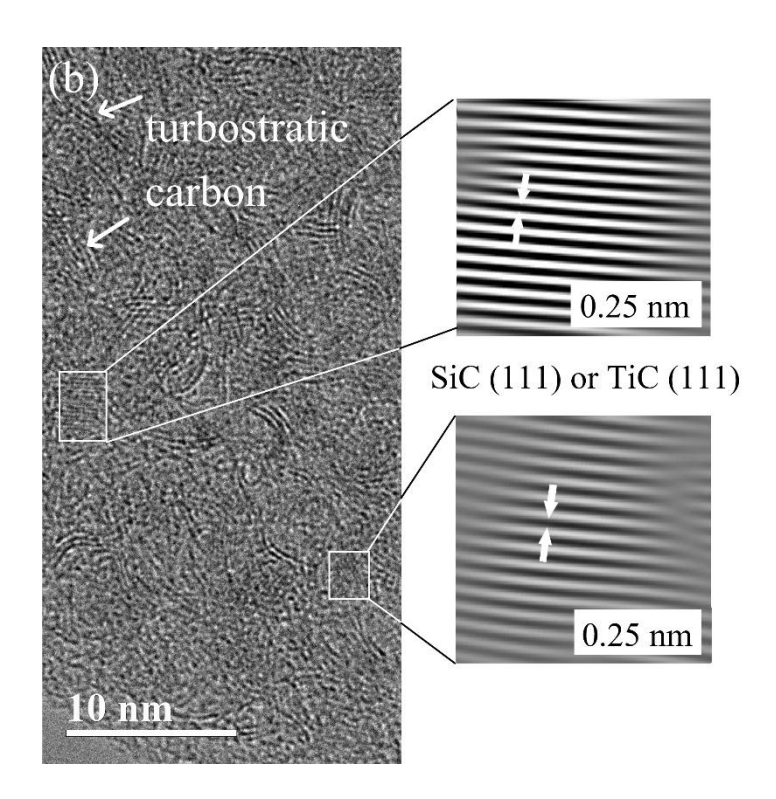


Fig. 4. Morphology of the SiOC–Ti-0.20 sample after pyrolysis at 1300 °C: (a) low magnification microstructure and largely amorphous diffraction pattern; (b) distribution of SiC and TiC nanocrystals in the SiOC matrix with the lattice fringe width shown.

## 3.3. Thermal stability

The high temperature oxidation stability of the Si-O-C-Ti samples is shown in Fig. 5. At 1200 °C pyrolysis temperature, the residual masses of all the samples are more than 99.80 wt%, except for the pure SiOC sample (93.90 wt%). There is a similar trend for the samples pyrolyzed at 1300°C. As the insert in Fig. 5(a) shows, there is a weight loss of 0.10 wt%, 0.16 wt%, 0.20 wt%, and 0.15 wt% for the SiOC-Ti-0.05, 0.10, 0.15, and 0.20 samples respectively from room temperature to 500 °C. This is due to the evaporation of moisture and carbon oxidation at low temperatures (400-800 °C), which causes a net weight loss for the resultant ceramic [29]:

$$C + O_2 \rightarrow CO_x$$
 (5)

As was discussed in our previous papers [3, 15], Eq. (5) involves oxidation of edge carbon atoms in the tiny graphene layers of the SiOC matrix, along with the oxidation of the radical species on the surface of free carbon.

Between 500 °C and 1000°C, weight gains up to 0.079 wt%, 0.11 wt%, and 0.12 wt% are observed for the SiOC-Ti-0.10, SiOC-Ti-0.15, and SiOC-Ti-0.20 samples. The oxidation of the Si-C bonds in the SiOC matrix leads to net weight gain, which can be described as:

$$Si-C + O_2 \rightarrow Si-O + CO_x$$
 (6)

The weight gain or loss depends on the oxidation rates of the excess carbon and the Si-C bonds in the SiOC matrix. Combining these two conflicting yet simultaneous reactions (5) and (6), and considering that TiC formation is minimal, it explains why only a small weight gain is observed for the samples pyrolyzed at 1200°C. Regardless, the high thermal stability of the SiOC-Ti-0.10, SiOC-Ti-0.15, and SiOC-Ti-0.20 samples after 1200 °C pyrolysis is clear. Compared to higher pyrolysis temperatures (1300 °C and 1400 °C), the amount of free carbon is relatively low in the SiOC matrix pyrolyzed at 1200 °C. Moreover, SiOC oxidation should be more vulnerable at higher temperatures (500 °C - 1000 °C) than at lower temperatures (< 500 °C), which results in the Si-C bond oxidation rate being comparable to that of the oxidation rate of carbon. This allows a SiO<sub>2</sub>-like surface to build up on SiOC based on reaction (6), which slows all subsequent reactions due to the necessity of O<sub>2</sub> diffusing in and CO<sub>x</sub> diffusing out for reactions (5) and (6) to occur. Regardless, it should be noted that the mass loss is relatively small for the Si-O-C-Ti samples compared to the pure SiOC system. This is because the possible reaction between TiO<sub>2</sub> and SiOC will induce more Si-C bonds from the amorphous SiOC phase due to the formation of SiO<sub>2</sub>:

$$TiO_2 + 2SiOC \rightarrow 2SiO_2 + TiC + C$$
 (7)

With more oxidation of the Si-C bonds in the SiOC matrix, less net weight loss occurs for the Si-O-C-Ti samples.

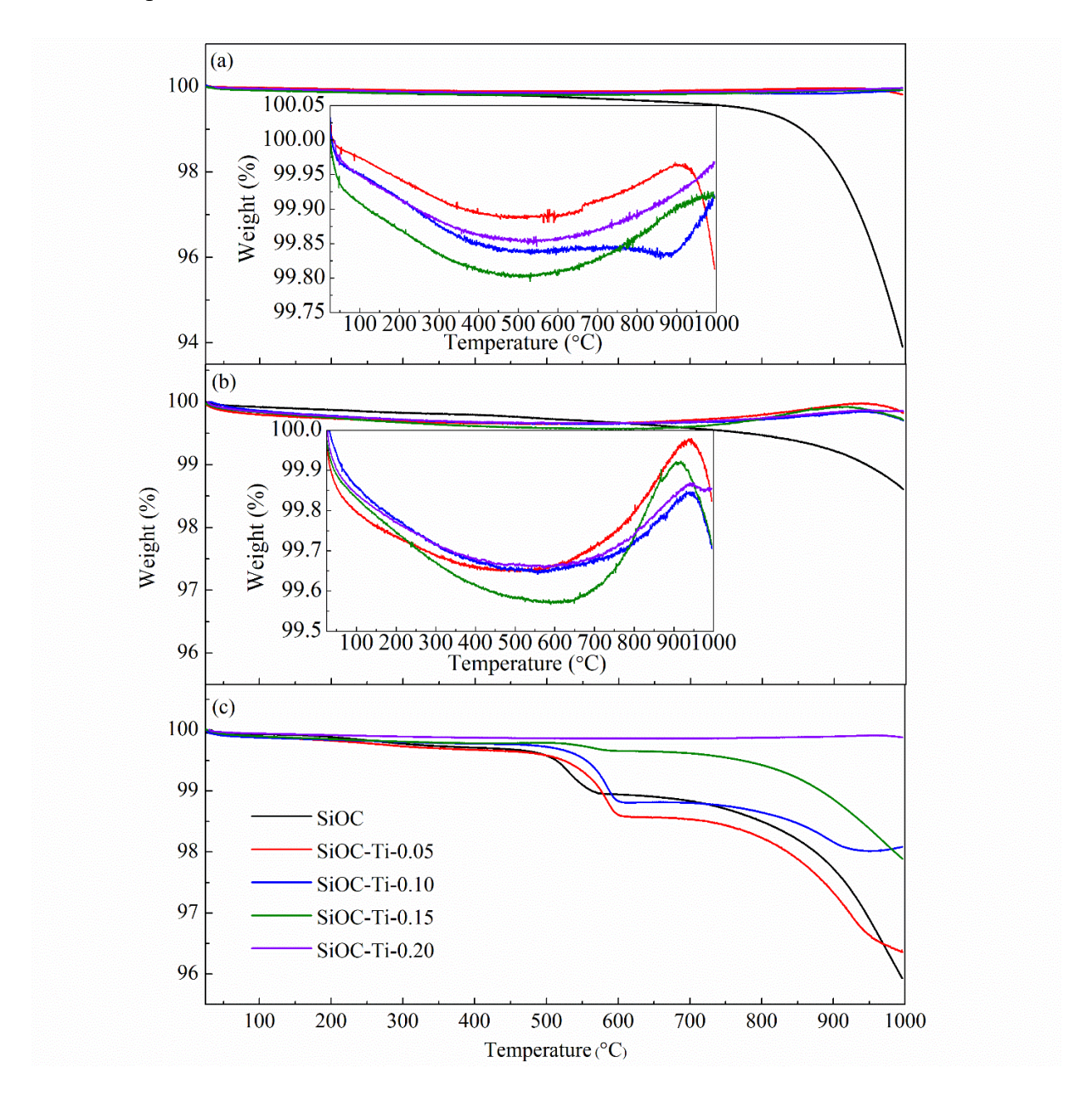


Fig. 5. TGA weight change curves in air for the pure SiOC and Si-O-C-Ti samples pyrolyzed at (a) 1200 °C, (b) 1300 °C, and (c) 1400 °C.

The above discussion also explains the "convex" shape of the weight curves in Fig. 5(a), that is, the net weight loss at lower temperatures and weight gain at higher temperatures. Unlike the other samples, only the weight of the SiOC-Ti-0.05 sample drops at 900°C. Based on reactions (1) and (2), less free carbon will be consumed to form TiC. Because of the higher amount of unreacted free carbon in the SiOC-Ti-0.05 sample than in the other samples, the oxidation of free carbon becomes more prominent once again from 900 °C to 1000 °C, resulting in weight loss (0.046 wt%). The residual masses of the SiOC-Ti-0.05, 0.20, 0.15, and 0.20 samples are 99.81 wt%, 99.91 wt%, 99.92 wt%, and 99.97 wt%, respectively. Higher TTIP content leads to higher thermal stability. This is because TiC is an extremely refractory ceramic material [30] and has a positive effect on the thermal stability.

At 1300 °C pyrolysis temperature, the residual mass for the pure SiOC sample is 96.16 wt%, and for the other samples they are all more than 99.70 wt%, as shown in Fig. 5(b). The thermal stability of all the Si-O-C-Ti samples is enhanced compared to the pure SiOC. Again, this is because TiC plays an active role in improving the thermal stability. At the same time, a mass loss of 3.84 wt% is observed for the pure SiOC sample between 600 °C and 1000 °C, indicating a continuous deterioration of the thermal stability due to carbon burning from 600 °C to 1000 °C [31]. However, this phenomenon is less extensive in the Si-O-C-Ti samples since part of the free carbon is consumed to support the conversion from TiO<sub>2</sub> to TiC (reaction (2)). Fig. 5(b) insert shows the convex-like curve, the same as in Fig. 5(a). The difference for the inserts in Figs. 5(a) and (b) is that a mass loss of 0.12 wt%, 0.11 wt%, and 0.20 wt% is detected for the SiOC-Ti-0.05, SiOC-Ti-0.10, SiOC-Ti-0.15 samples respectively from 900 °C to 1000 °C. It has been explained by the less carbon consumption in the lower TTIP-containing samples through the reduction reaction (2), which makes the oxidation of free carbon more prominent at a higher

temperature and results in mass loss after 900°C. In Fig. 5(b), the above phenomenon occurs in all the Si-O-C-Ti samples except for SiOC-Ti-0.20. In Fig. 5(a), the exception is only SiOC-Ti-0.05. Higher pyrolysis temperature promotes more free carbon phase. At 1300 °C, more free carbon in the matrix results in more prominent carbon oxidation (mass loss) than at 1200°C. It also explains why more samples have mass loss at a later stage in Fig. 5(b). The TTIP content effect is the same as at 1200°C. Higher TiC content means higher thermal stability.

Fig. 5(c) shows no convex line in the mass change curves. Only mass loss from 500 °C to 1000 °C occurs. The pure SiOC sample still shows the lowest thermal stability (95.93 wt%). The residual masses of the SiOC-Ti-0.05, 0.10, 0.15, and 0.20 samples are 96.36 wt%, 98.08 wt%, 97.89 wt%, and 99.88 wt%, consistent with the observation that the thermal stability is proportional to the TiC content. All the samples show mass loss because of the more extensive phase separation and free carbon formation at 1400 °C. The samples pyrolyzed at 1400 °C are less stable because the pyrolysis process consumes more free carbon and 'destabilizes' the SiOC system. As we have discussed at the beginning of this section, TiC is an extremely refractory material. Higher TiC samples mean higher thermal stability.

Table 3 shows that the mass loss after 1000 °C thermal treatment in air for 25 h varies from 23.25 to 36.96 wt%. The reasons have been detailed above with extended thermal exposure. However, no weight loss is detected for all the samples during the period of 25-100 h thermal treatment. This means that after the initial mass loss, the Si-O-C-Ti system has superior thermal stability, and higher TiC content results in higher thermal stability.

Table 3. Mass loss of different SiOC-Ti samples with different dwelling time at 1000°C.

<b>Pyrolysis</b>	Mass loss (wt%)

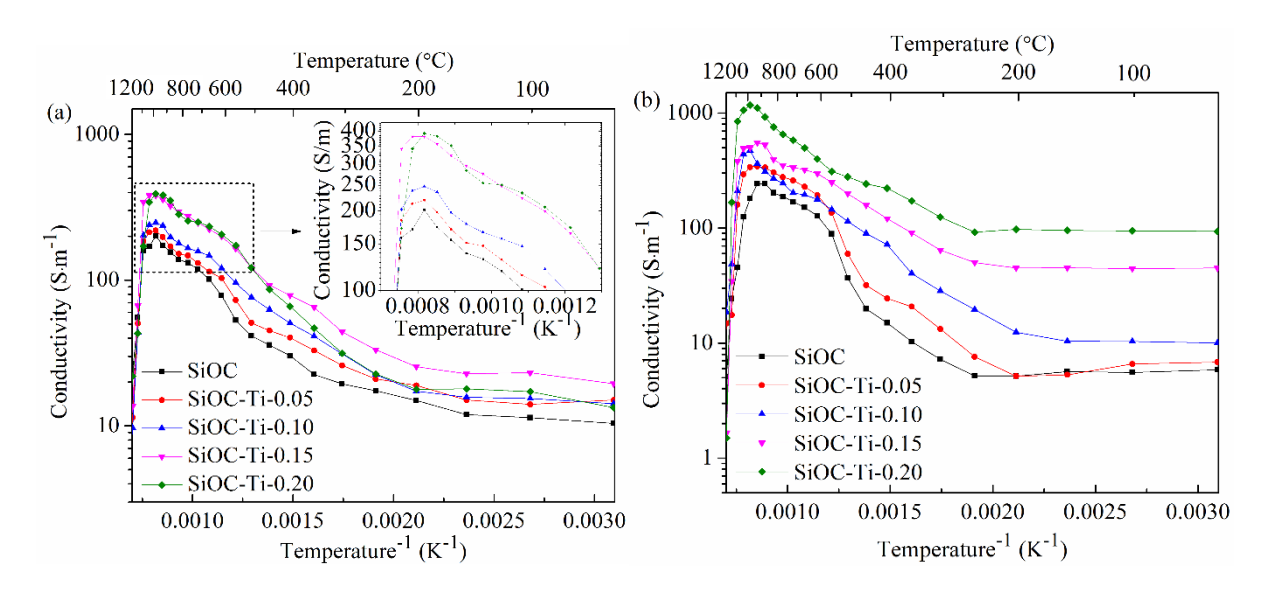
temperature	Sample	0-25 h	25-50 h	50-75 h	75-100 h
	SiOC	$36.89\pm2.15$	0	0	0
	SiOC-Ti-0.05	$35.62\pm1.74$	0	0	0
1200 °C	SiOC-Ti-0.10	$35.55\pm2.16$	0	0	0
	SiOC-Ti-0.15	$29.74 \pm 0.98$	0	0	0
	SiOC-Ti-0.20	$23.49 \pm 1.26$	0	0	0
	SiOC	$36.74\pm0.63$	0	0	0
	SiOC-Ti-0.05	35.28±1.79	0	0	0
1300 °C	SiOC-Ti-0.10	$32.71\pm2.16$	0	0	0
	SiOC-Ti-0.15	$24.02\pm0.46$	0	0	0
	SiOC-Ti-0.20	$23.25\pm1.02$	0	0	0
	SiOC	36.96±1.39	0	0	0
	SiOC-Ti-0.05	$32.87\pm2.51$	0	0	0
1400 °C	SiOC-Ti-0.10	$33.31 \pm 0.78$	0	0	0
	SiOC-Ti-0.15	$30.42\pm1.21$	0	0	0
	SiOC-Ti-0.20	29.36±1.59	0	0	0

## 3.4. Electrical conductivity

Fig. 6 shows the electrical conductivity changes for the SiOC samples pyrolyzed at 1200-1400 °C with different amount of TTIP addition.

At 1200 °C pyrolysis temperature (Fig. 6(a)), for the pure SiOC sample, the conductivity increases from 10.39 to 201.49 S/m from room temperature to 950 °C, then decreases to 3.29 S/m at 1200 °C. Based on the literature [32], decomposition of hydrocarbon fragments resulting

from the cleavage of the functional groups bonded to silicon (e.g., Si–C<sub>6</sub>H<sub>5</sub>, Si–CH<sub>3</sub>) leads to the precipitation of turbostratic carbon clusters, which are the main contributor to the electrical conductivity of Si-O-C ceramics. For SiOC-Ti-0.05, the conductivity ranges from 34.02 S/m at 50 °C to 0.15 S/m at 1200 °C and achieves the highest electrical conductivity of 232.92 S/m at 900°C. Compared to the pure SiOC, the increasing conductivity is a result of additional TiC (3.3x10<sup>6</sup> S/m, 20 °C [33]) formation and free (segregated) carbon content, which has been validated by our previous work [15]. With more TiC formation, the conductivity generally shows an increase from SiOC-Ti-0.05 to SiOC-Ti-0.20, although no obvious difference is observed between SiOC-Ti-0.15 and SiOC-Ti-0.20. As mentioned in our earlier work [15], the conversion from TTIP to TiC can lead to an increased free carbon content as well as structural transformation of sp<sup>3</sup> carbon into sp<sup>2</sup> carbon. The ordering, amount, and interconnectivity of the carbon network exert a major influence on the electrical conductivity [34, 35]. A higher fraction of carbon with sp<sup>2</sup> bonds leads to higher conductivity for the pyrolyzed materials.



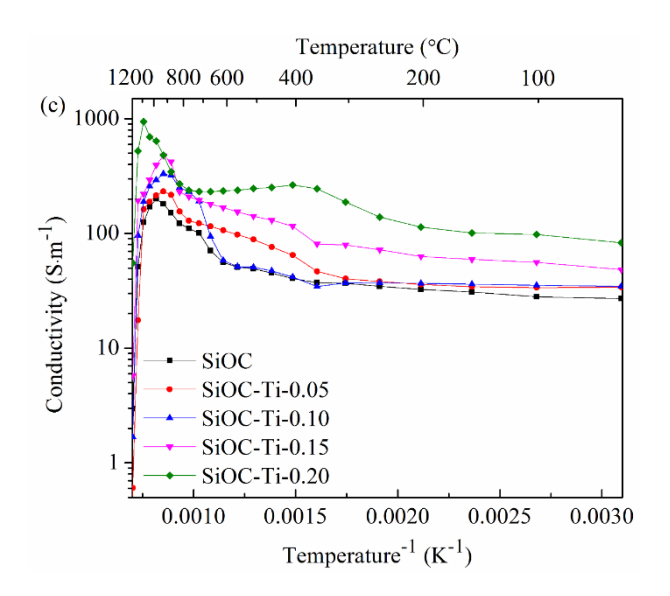


Fig. 6. Electrical conductivity for the SiOC, SiOC-Ti-0.05, SiOC-Ti-0.10, SiOC-Ti-0.15, and SiOC-Ti-0.20 samples after different pyrolysis temperatures in an argon atmosphere.

At 1300 °C pyrolysis temperature, the electrical conductivity of the pure SiOC increases from 5.85 S/m (50 °C) to 243.53 S/m (850 °C) before decreasing to 0.94 S/m (1200 °C). An increase is observed when compared to that of the 1200 °C pyrolysis temperature. This means that higher temperature promotes carbon cluster growth; edge-to-edge linkage of neighboring structural units may coalesce to form an interconnected network (cluster size to infinity) of turbostratic carbon ribbons in the matrix [36]. As for the Si-O-C-Ti system, the electrical conductivity still increases with the TTIP content. This has been explained based on increased carbon ordering, which can be confirmed by the Raman data shown in Fig. 7 for selected samples pyrolyzed at 1300 °C. The two Lorentzian peaks at ~1350 cm<sup>-1</sup> and 1580 cm<sup>-1</sup> are assigned to the D band and G band, respectively. The D' peak centered at 1540 cm<sup>-1</sup> is from the amorphous carbon structure [37]. Good curve fitting results (R<sup>2</sup>>0.95) are achieved. The decreasing peak area ratio (A<sub>D</sub>/A<sub>G</sub> from 4.21 to 3.19 from the pure SiOC sample to the SiOC-Ti-0.20 sample) and the disappearance of the D' band are important indications of a higher degree

of crystallization for the carbon structure in the Si-O-C-Ti samples. It is worth noting that SiOC-Ti-0.20 achieves the highest electrical conductivity of 1176.55 S/m at 950 °C. To our best knowledge, it is the first report that the conductivity for Si-O-C-Ti ceramics is over 1000 S/m. In the previous study [15], we in situ synthesized silicon oxycarbide (SiOC)–TiC<sub>x</sub>O<sub>y</sub> composites based on the pyrolysis of polysiloxane and carbothermal reaction between TiO<sub>2</sub> nanoparticles and free carbon in SiOC. However, the conductivity of the SiOC–TiC<sub>x</sub>O<sub>y</sub> composites is suppressed to a certain degree because of the heterogeneous dispersion of the TiO<sub>2</sub> particles in the polymeric precursor. In this study, the incorporation of titanium isopropoxide, which is an organic compound completely miscible with the polysiloxane, addresses the inhomogeneity issue; the electrical conductivity of the SiOC–Ti-0.20 sample is further improved.

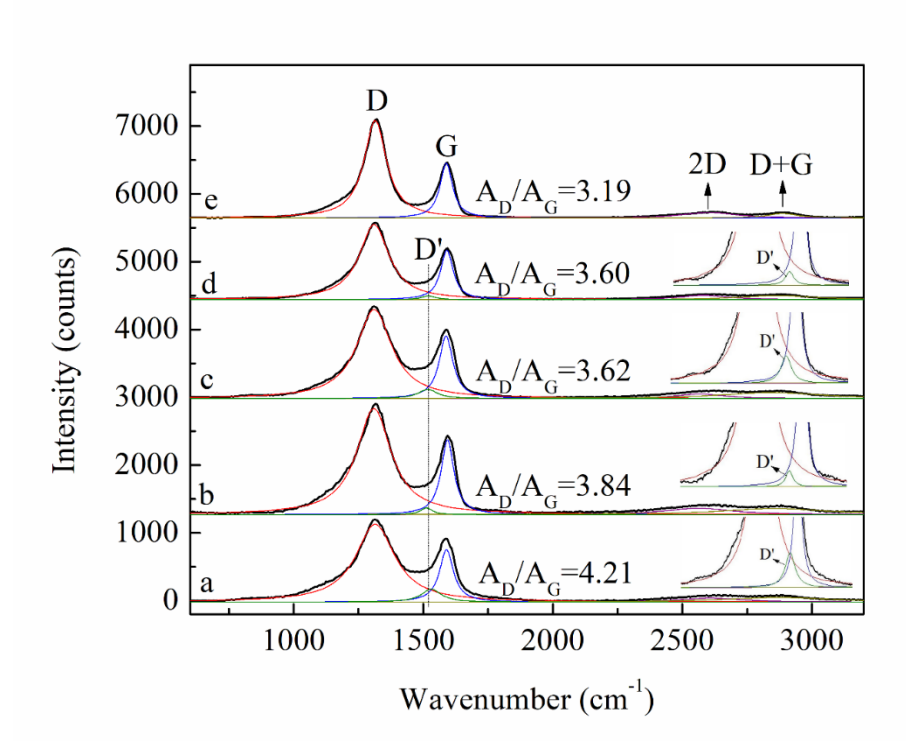


Fig. 7. Curve-fitting Raman spectra of different samples pyrolyzed at 1300 °C for (a) SiOC, (b) SiOC-Ti-0.05, (c) SiOC-Ti-0.10, (d) SiOC-Ti-0.15, and (e) SiOC-Ti-0.20 samples.

At 1400 °C pyrolysis temperature, Fig. 6(c) shows that the overall conductivity for the SiOC-Ti samples is lower than that of 1300°C. The maximum value, from SiOC-Ti-0.20, is measured to be 946.07 S/m. With more TiC formation (Fig. 2), higher pyrolysis temperature should lead to higher electrical conductivity. However, the electrical conductivity of the Si-O-C-Ti samples is also dependent on the ordering, content, and interconnectivity of the carbon network. Higher pyrolysis temperature intensifies the carbothermal reaction between TiO<sub>2</sub> and carbon (Eq. (2)) and damages the interconnectivity of the carbon network, which results in lower conductivity values. It also means that too high and too low pyrolysis temperatures are not conductive to high conductivity. At higher measurement temperatures than 850-950 °C, all the samples (Fig. 6) show a drastic conductivity decrease. This is caused by the breakdown of the conductive turbostratic carbon network under the electric field as well as the formation of a surface oxide layer [3, 15]. Also, the silver/palladium paste used as electrodes starts to thermally decompose at around 1000 °C. Higher-temperature resistant paste is still pursued in our study.

#### 4. Conclusions

This work focuses on using a titanium complex as an additive to synthesize superior thermal stability and high electrical conductivity Si-O-C-Ti ceramics. The volume shrinkage is 41-64.5%, the ceramic yield is 61.2-76.6%, and the resultant Si-O-C-Ti composite density is 1.8-2 g/cm<sup>3</sup>. TTIP conversion to TiC increases with the increase of the pyrolysis temperature by carbothermal reaction. Unlike pure SiOC, all the Si-O-C-Ti composites pyrolyzed at 1200 and 1300 °C are thermally stable up to 1000 °C in air with >99.80 wt% mass retention. However, these Si-O-C-Ti samples at 1400 °C pyrolysis temperature are less stable, especially when they consume the free carbon and 'destabilize' the SiOC system. The electrical conductivity increases

from room temperature to ~950 °C and then decreases due to the breakdown of the conductive path from the turbostratic carbon network. The maximum conductivity of 1176.55 S/m is achieved by SiOC-Ti-0.20 pyrolyzed at 1300 °C at 950 °C, in argon, which is the highest reported for the SiOC-based systems. The conductivity of the Si-O-C-Ti composites is related to the ordering, amount, and interconnectivity of the carbon network as well as TiC formation.

## **Acknowledgment:**

We acknowledge the financial support from National Science Foundation under grant number CMMI-1634325 and Department of Energy under the grant number DE-NE 0008807.

#### References

- [1] K. Lu, Porous and high surface area silicon oxycarbide-based materials—a review, Mater. Sci. Eng. R Rep. 97 (2015) 23-49.
- [2] E. Ionescu, H.-J. Kleebe, R. Riedel, Silicon-containing polymer-derived ceramic nanocomposites (PDC-NCs): Preparative approaches and properties, Chem. Soc. Rev. 41(15) (2012) 5032-5052.
- [3] K. Lu, D. Erb, M. Liu, Thermal stability and electrical conductivity of carbon-enriched silicon oxycarbide, J. Mater. Chem. C 4(9) (2016) 1829-1837.
- [4] C. Stabler, E. Ionescu, M. Graczyk- Zajac, I. Gonzalo- Juan, R. Riedel, Silicon oxycarbide glasses and glass- ceramics: "All- rounder" materials for advanced structural and functional applications, J. Am. Ceram. Soc. 101(11) (2018) 4817-4856.

- [5] R. Corriu, D. Leclercq, P. Mutin, A. Vioux, <sup>29</sup>Si nuclear magnetic resonance study of the structure of silicon oxycarbide glasses derived from organosilicon precursors, J. Mater. Sci. 30(9) (1995) 2313-2318.
- [6] R. Zhuo, P. Colombo, C. Pantano, E.A. Vogler, Silicon oxycarbide glasses for blood-contact applications, Acta Biomater. 1(5) (2005) 583-589.
- [7] H.-F. Li, S. Dimitrijev, D. Sweatman, H. Harrison, Effect of NO annealing conditions on electrical characteristics of n-type 4H-SiC MOS capacitors, J. Electron. Mater. 29(8) (2000) 1027-1032.
- [8] Y. Ding, H. Shirai, White light emission from silicon oxycarbide films prepared by using atmospheric pressure microplasma jet, J. Appl. Phys. 105(4) (2009) 043515.
- [9] R. Riedel, L. Toma, E. Janssen, J. Nuffer, T. Melz, H. Hanselka, Piezoresistive effect in SiOC ceramics for integrated pressure sensors, J. Am. Ceram. Soc. 93(4) (2010) 920-924.
- [10] L. David, R. Bhandavat, U. Barrera, G. Singh, Silicon oxycarbide glass-graphene composite paper electrode for long-cycle lithium-ion batteries, Nat. Commun. 7 (2016) 10998.
- [11] Y.D. Blum, D.B. MacQueen, H.-J. Kleebe, Synthesis and characterization of carbon-enriched silicon oxycarbides, J. Eur. Ceram. Soc. 25(2-3) (2005) 143-149.
- [12] G.D. Sorarù, D. Suttor, High temperature stability of sol-gel-derived SiOC glasses, J. Sol-Gel Sci. Technol. 14(1) (1999) 69-74.
- [13] G.D. Sorarù, Q. Liu, L.V. Interrante, T. Apple, Role of precursor molecular structure on the microstructure and high temperature stability of silicon oxycarbide glasses derived from methylene-bridged polycarbosilanes, Chem. Mater. 10(12) (1998) 4047-4054.

- [14] T. Erny, M. Seibold, O. Jarchow, P. Greil, Microstructure development of oxycarbide composites during active-filler-controlled polymer pyrolysis, J. Am. Ceram. Soc. 76(1) (1993) 207-213.
- [15] K. Lu, D. Erb, M. Liu, Phase transformation, oxidation stability, and electrical conductivity of TiO<sub>2</sub>-polysiloxane derived ceramics, J. Mater. Sci. 51(22) (2016) 10166-10177.
- [16] K. Lu, D. Erb, Polymer derived silicon oxycarbide-based coatings, Int. Mater. Rev. 63(3) (2018) 139-161.
- [17] S.-H. Kim, Y.-W. Kim, C. Park, Effect of inert filler addition on pore size and porosity of closed-cell silicon oxycarbide foams, J. Mater. Sci. 39(10) (2004) 3513-3515.
- [18] Y.W. Kim, J.H. Eom, C. Wang, C.B. Park, Processing of porous silicon carbide ceramics from carbon-filled polysiloxane by extrusion and carbothermal reduction, J. Am. Ceram. Soc. 91(4) (2008) 1361-1364.
- [19] S.-H. Chae, Y.-W. Kim, Effect of inert filler addition on microstructure and strength of porous SiC ceramics, J. Mater. Sci. 44(5) (2009) 1404-1406.
- [20] E. Ionescu, C. Linck, C. Fasel, M. Müller, H.J. Kleebe, R. Riedel, Polymer-derived SiOC/ZrO<sub>2</sub> ceramic nanocomposites with excellent high-temperature stability, J. Am. Ceram. Soc. 93(1) (2010) 241-250.
- [21] E. Ionescu, B. Papendorf, H.J. Kleebe, R. Riedel, Polymer- derived silicon oxycarbide/hafnia ceramic nanocomposites. Part II: Stability toward decomposition and microstructure evolution at T>> 1000 °C, J. Am. Ceram. Soc. 93(6) (2010) 1783-1789.
- [22] R. Harshe, C. Balan, R. Riedel, Amorphous Si (Al) OC ceramic from polysiloxanes: bulk ceramic processing, crystallization behavior and applications, J. Eur. Ceram. Soc. 24(12) (2004) 3471-3482.

- [23] X. Yan, D. Su, H. Duan, F. Zhang, Preparation of SiOC/HfO<sub>2</sub> fibers from silicon alkoxides and tetrachloride hafnium by a sol–gel process, Mater. Lett. 148 (2015) 196-199.
- [24] V.G. Nguyen, H. Thai, D.H. Mai, H.T. Tran, M.T. Vu, Effect of titanium dioxide on the properties of polyethylene/TiO<sub>2</sub> nanocomposites, Composites Part B 45(1) (2013) 1192-1198.
- [25] V. Gourinchas Courtecuisse, K. Chhor, J.-F. Bocquet, C. Pommier, Kinetics of the titanium isopropoxide decomposition in supercritical isopropyl alcohol, Ind. Eng. Chem. Res. 35(8) (1996) 2539-2545.
- [26] L.-M. Berger, W. Gruner, E. Langholf, S. Stolle, On the mechanism of carbothermal reduction processes of TiO<sub>2</sub> and ZrO<sub>2</sub>, Int. J. Refract. Met. Hard Mater. 17(1-3) (1999) 235-243. [27] D. Tan, Z. Ma, B. Xu, Y. Dai, G. Ma, M. He, Z. Jin, J. Qiu, Surface passivated silicon

nanocrystals with stable luminescence synthesized by femtosecond laser ablation in solution, Phys. Chem. Chem. Phys. 13(45) (2011) 20255-20261.

- [28] K. Lu, J. Li, Fundamental understanding of water vapor effect on SiOC evolution during pyrolysis, J. Eur. Ceram. Soc. 36(3) (2016) 411-422.
- [29] C.M. Brewer, D.R. Bujalski, V.E. Parent, K. Su, G.A. Zank, Insights into the oxidation chemistry of SiOC ceramics derived from silsesquioxanes, J. Sol-Gel Sci. Technol. 14(1) (1999) 49-68.
- [30] D. Vallauri, I.A. Adrian, A. Chrysanthou, TiC–TiB<sub>2</sub> composites: a review of phase relationships, processing and properties, J. Eur. Ceram. Soc. 28(8) (2008) 1697-1713.
- [31] D. Tang, J. Su, Q. Yang, M. Kong, Z. Zhao, Y. Huang, X. Liao, Y. Liu, Preparation of alumina-coated graphite for thermally conductive and electrically insulating epoxy composites, RSC Adv. 5(68) (2015) 55170-55178.

- [32] J. Cordelair, P. Greil, Electrical conductivity measurements as a microprobe for structure transitions in polysiloxane derived Si–O–C ceramics, J. Eur. Ceram. Soc. 20(12) (2000) 1947-1957.
- [33] Y. Pang, H. Xie, R. Koc, Investigation of electrical conductivity and oxidation behavior of TiC and TiN based cermets for SOFC interconnect application, ECS Trans. 7(1) (2007) 2427-2435.
- [34] E. Bouillon, F. Langlais, R. Pailler, R. Naslain, F. Cruege, P. Huong, J. Sarthou, A. Delpuech, C. Laffon, P. Lagarde, Conversion mechanisms of a polycarbosilane precursor into an SiC-based ceramic material, J. Mater. Sci. 26(5) (1991) 1333-1345.
- [35] G.M. Renlund, S. Prochazka, R.H. Doremus, Silicon oxycarbide glasses: Part I. Preparation and chemistry, J. Mater. Res. 6(12) (1991) 2716-2722.
- [36] M. Monthioux, O. Delverdier, Thermal behavior of (organosilicon) polymer-derived ceramics. V: Main facts and trends, J. Eur. Ceram. Soc.16(7) (1996) 721-737.
- [37] X. He, X. Liu, B. Nie, D. Song, FTIR and Raman spectroscopy characterization of functional groups in various rank coals, Fuel 206 (2017) 555-563.